Comparison of IR properties of two classes of Seyfert 2 galaxies – with and without broad lines in polarized light

Georgi P. Petrov
Department of Astronomy, Faculty of Physics, University of Sofia, Bulgaria
g_petrov@phys.uni-sofia.bg
(Conference poster. Accepted on 21.12.2009)

Abstract. We have compiled a sample of 82 Seyfert 2 objects with and without detected polarized broad emission lines. For each object we have done a 2MASS photometry in J, H, K_S bands in 6 arcsec aperture. Our goal is to determine the properties of these two apparently different populations of Seyfert 2 galaxies. For this purpose we have used color – color diagram (J–H) – (H–K_S) and gas to dust ratio defined by the flux of the emission line [OIII] λ5007 to the flux the in the K_S band of the central source. These parameters are closely related to the strength of the active nucleus luminosity compared to the host galaxy luminosity. Both indicate the influence of the nuclear obscuration.

We have found that the Seyfert 2 galaxies with polarized broad emission lines reveal infrared properties similar to the Seyfert 1 galaxies and the objects without polarized broad emission lines show infrared properties almost like normal galaxies. According to our results, Seyfert 2 galaxies with polarized broad lines have typically higher $F_{[OIII]}/F_{K_S}$ ratios than those without. The objects without detected polarized broad lines have a central source highly obscured by dust and some of them possess an intrinsically weak central engine.
Key words: galaxies: active, galaxies: Seyfert, polarization

Свойства на Сийфърт 2 галактиките с и без наличие на поляризирани емисионни линии с широки крила

Георги П. Петров

Направена е извадка от 82 Сийфърт 2 галактики с и без наличие на наблюдавани поляризирани емисионни линии с широки крила. За всеки от обектите е направена 2MASS фотометрия в J, H, K_S филтри в 6 arcsec апертура. Целта е да се определят свойствата на тези два, видимо различни, типа Сийфърт 2 галактики. За тази цел са използвани диаграмата (J–H) – (H–K_S) и отношението газ-прах, определено от потока в линията [OIII] λ5007, съотнесено към потока във филтъра K_S, излъчван от ядрото на галактиката. Тези параметри показват доколко светимостта на ядрото доминира спрямо тази на родителската галактика. Те отчитат и скриването на ядрото от праха.

Установихме, че Сийфърт 2 галактиките с наличие на поляризирани емисионни линии с широки крила проявяват инфрачервени свойства подобни на Сийфърт 1 галактиките. Сийфърт 2 галактиките без наблюдавани поляризирани линии с широки крила проявяват инфрачервени свойства по-близки до тези на нормалните галактики. Съгласно нашите резултати, Сийфърт 2 обектите с наблюдавани поляризирани линии с широки крила обикновено имат по-високи $F_{[OIII]}/F_{K_S}$ отколкото обектите без такива емисионни линии. Последните показват значително закрито от прах ядро, а някои от тях имат слаб централен източник.

1 Introduction

The standard theory of active galaxies is based on the idea of an accretion disk around a massive black hole (BH). This engine powers the hard X-ray

continuum which is strong enough to photoionize the Broad Line Region (BLR) placed near the source and the Narrow Line Region (NLR) which is located farther away from the nucleus.

According to the basic assumption of the Unified model, Seyfert galaxies are divided into types 1 and 2, which are intrinsically the same objects and differ only in their orientation with respect to the observer (Antonucci 1993). The main reason for the apparent difference is the presence of an optically thick torus around the nucleus and the BLR. To see Seyfert 2 (Sy2) type galaxies, we observe the torus edge-on and all emission from the BLR is obscured by this molecular torus, while the narrow lines are still visible. On the other hand, for Seyfert 1 (Sy1) type objects our line of sight is perpendicular to the torus and the nucleus and the BLR are visible.

Important observational evidence to support the hypothesis of the Unified model is the detection of polarized broad emission lines (PBLs) in Sy2 galaxies (Antonucci and Miller 1985). In fact, a large fraction of Sy2 objects do not show PBLs in the spectropolarimetric observations.

On the other hand, in the framework of the Unified model the column density of neutral hydrogen $N_{\rm H}$ defined by the X–ray absorption in Sy2s is significantly higher than that in type 1 objects due to the presence of a torus which is along the line of sight. As an exception from this model Panessa and Bassani (2002) found a group of Sy2 galaxies that appear to be unabsorbed in X–rays and their measured column densities are $N_{\rm H} < 10^{22}$ cm^{-2}.

There are several possible reasons for the absence of the PBLs in some Sy2 galaxies:

- They simply don't harbour a BLR (Tran 2001, 2003).
- The absence of PBLs corresponds to low values of accretion rate (Nicastro et al. 2003).
- The detectability of PBLs is mainly determined by the relative luminosity of the active nucleus to the host galaxy (Lumsden et al. 2001).
- The visibility of PBLs is significantly determined by the nuclear obscuration (Shu et al. 2007, 2008).

In this paper we have studied a sample of 82 Sy2 objects with and without detected PBLs. For each object we have performed a 2MASS photometry in J, H, K_S bands in 6 arcsec aperture. To determine the properties of these two apparently different fractions of Sy2 galaxies, we have used color – color diagram (J–H) – (H–K_S) and gas to dust ratio defined by the flux of the emission line [OIII] λ5007 to the flux the in the K_S band (in 6 arcsec aperture) of the central core. These parameters are closely related to the strength of the active nucleus luminosity compared to the host galaxy luminosity and indicate the influence of the nuclear obscuration.

2 Data and results

Our sample contains 82 Sy2 galaxies and most of them are classified by NED as Sy 2 type, but others - as type 1.8 – 1.9. For the sake of simplicity, we

generally call them Sy2. In this paper we adopt the Hubble constant H_0= 75 km s^{-1} Mpc^{-1} as all objects are low-z.

We have used Sy2 galaxies with spectropolarimetric observations from the sample of Shu et al. (2007). They made their total sample collecting spectropolarimetric data mainly from several large surveys (Heisler et al. 1997, Lumsden et al. 2001, Moran et al. 2000, 2001, Tran et al. 2001, Young et al. 1996). For 82 Sy2s of the sample of Shu et al. (2007) we have done a 2MASS photometry in 6 arcsec aperture based on the available images in J, H, Ks bands for these objects [1]. Thus, our sample contains 34 Sy2 galaxies with PBLs and the rest 48 Sy2s are without detected PBLs. For our photometric measurements we have used 2MASS Atlas images with 120 arcsec size. For each object we have done a photometry of the central 6 arcsec of the galaxy using IDL. This is smallest possible aperture and it is three times the 2MASS seeing. To avoid mistakes due to contamination by close objects we have made a calibration using a linear approximation of our J, H, K_S in 6 arcsec aperture to the very accurate 2MASS J, H, K_S magnitudes in 14 arcsec aperture from NED.

$$J_6 = J_{14} \times 0.89 + 2.12 \quad \text{with } \sigma = 0.19, \tag{1}$$

$$H_6 = H_{14} \times 0.90 + 1.84 \quad \text{with } \sigma = 0.21, \tag{2}$$

$$K_{S6} = K_{S14} \times 0.94 + 1.33 \text{ with } \sigma = 0.25, \tag{3}$$

where σ is the rms of residuals.

The magnitudes in J, H, K_S bands (6 arcsec aperture) for the Sy2s with and without PBLs are shown in Table 1.

2.1. Color – color diagram (J–H) – ($H–K_S$)

To reveal the differences between the Sy2s with and without PBLs we have used color – color diagram (J–H) – ($H–K_S$). In Fig.1 can be seen two oval regions. The first one is centered at (J–H) = 0.77, ($H–K_S$) = 0.26 and represents the region populated by normal galaxies, without any signs of activity (Willner et al. 1984). The second one is centered at (J–H) = 0.95, ($H–K_S$) = 1.15 and it is populated by quasars after the redshift correction (Hyland and Allen 1982). The space between the two oval regions is populated by active galaxies. According to Kotilainen et al. (1992), Sy1 galaxies are located near the quasars' area on the diagram. In our case most of the Sy2 galaxies with PBLs are located close to the usual area of Sy1's. On the other hand, the Sy2 galaxies without PBLs are mainly located closer to the region populated by normal galaxies. This fact could be interpreted as evidence that the Sy2 galaxies without PBLs are more obscured than those with PBLs. This obscuration of the central source is the reason for the bigger contribution of the host galaxy luminosity. The dashed line in Fig.1 is the black body locus for different temperatures and the location of the Sy2's without PBL's near it shows that the contribution of the host galaxy luminosity is significant for

[1] http://irsa.ipac.caltech.edu

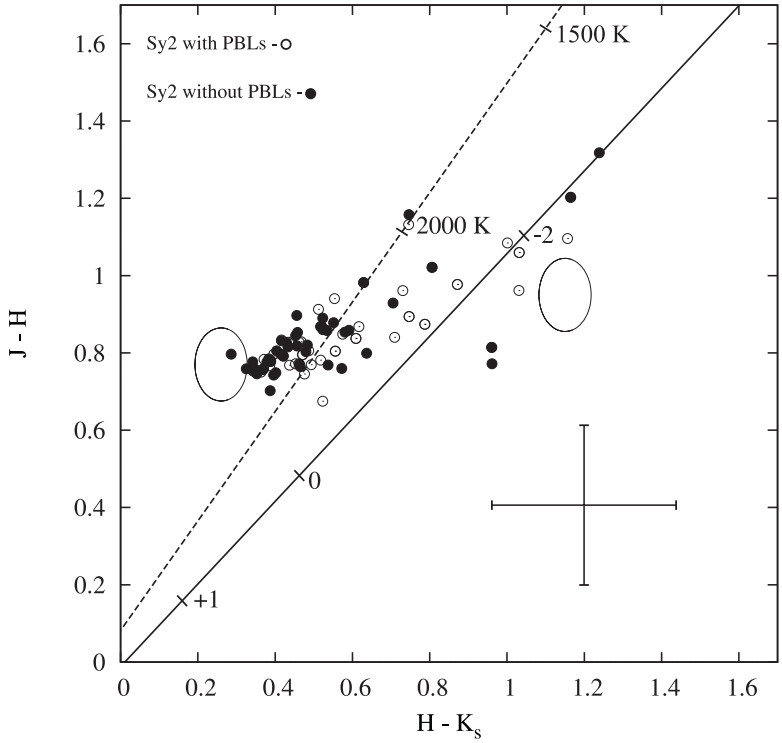

Fig. 1. (J–H) vs. (H–K_S) diagram. Oval regions represent areas populated by normal galaxies and quasars (see the text). The solid line is the power-law locus with marked spectral indices. The dashed line is the black body locus for different temperatures. The Sy2 objects with PBLs are shown as open circles. Filled circles represent the Sy2 galaxies without PBLs. The standard error is plotted in the bottom - left corner of the diagram.

these objects. In the case of the Sy2's with PBL's there is a clearly dominating central source and these objects are mainly located close to the solid line, which presents the power-law locus with various spectral indices.

2.2. Gas to dust ratio

The difference in the central source obscuration between the two populations of Sy2s may be explained with different values of the gas-to-dust ratio. This ratio is well represented by $F_{[OIII]}/F_{\mathrm{K_S}}$ ratio. The flux $F_{[OIII]}$ (λ5007) is an indicator for the gas contents in the centre of the active galaxy. At the same time, the flux $F_{\mathrm{K_S}}$ in the K_S-band originates from thermal emission of dust grains in the optically thick torus. The sublimation temperature of graphite grains is in the range 1500 - 1800 K. From Wien's law, $T\lambda_{peak}(\mu\mathrm{m}) = 2898$, so the peak wavelength of re-radiation from the dusty torus should be around 2μm (Peng et al. 2006).

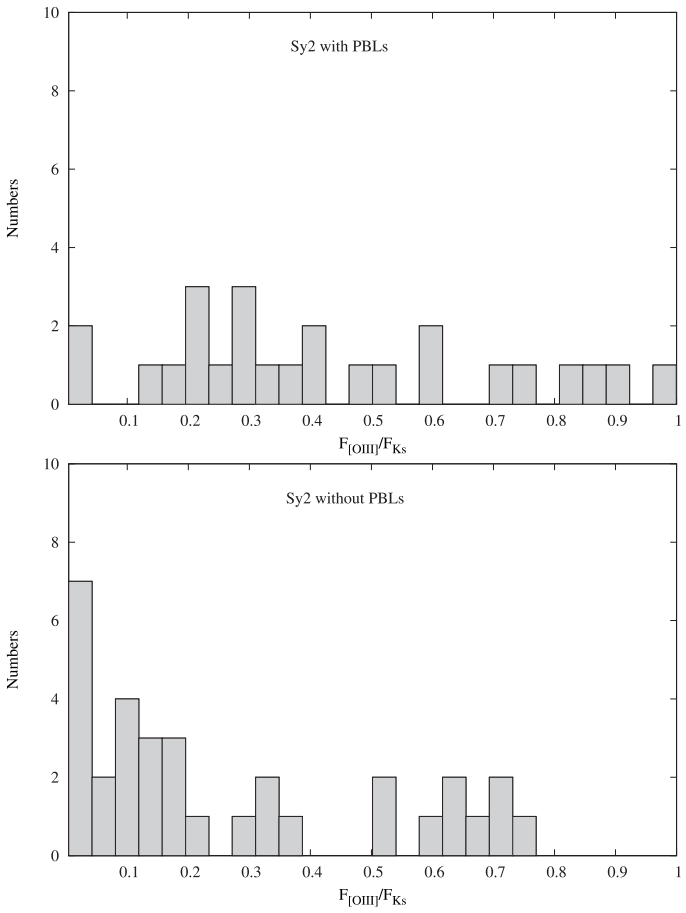

Fig. 2. $F_{[OIII]}/F_{\rm Ks}$ histograms for the two populations of Sy2 galaxies.

For our purpose we have collected the observed fluxes $F^{obs}_{[OIII]}$ (λ5007) from literature (see Table 1). We have obtained data about these fluxes for 30 Sy2 objects with PBL's of our sample and for 38 Sy2's without PBL's. These fluxes have been extinction corrected assuming an intrinsic Balmer decrement $(H_\alpha/H_\beta)_0 = 3.1$.

In Fig.2 we have plotted two histograms. They present the distribution of the $F_{[OIII]}/F_{\rm Ks}$ ratios for Sy2 galaxies with PBLs and without PBLs. The two histograms show the ratio values below 1.0, where the differences in the distribution between the two types Sy2s are significant. The mean value for the Sy2s with PBLs is $F_{[OIII]}/F_{\rm Ks} = 0.44$ and the standard deviation of the sample is SD = 0.28. For the objects without PBLs the mean value is $F_{[OIII]}/F_{\rm Ks} = 0.27$ and SD = 0.25. We have used a two-sample Kolmogorov-

Smirnov (K-S) test. The K-S statistic is DN = 0.46, which corresponds to a P-value = 0.005 and as the value is lower than 0.01, there is significant difference between the distributions at 99% confidence level. In this case, the Sy2 objects with $F_{[OIII]}/F_{\mathrm{K_S}} > 1$ were excluded because they have unusually high $F_{[OIII]}$ fluxes in comparison to most of the other objects. We have performed another test including all objects with available $F_{[OIII]}/F_{\mathrm{K_S}}$ ratios. The mean value for the Sy2s with PBLs is $F_{[OIII]}/F_{\mathrm{K_S}} = 1.12$ and SD = 2.25. For the objects without PBLs the mean value is $F_{[OIII]}/F_{\mathrm{K_S}} = 0.44$ and SD = 0.54. The K-S statistic is DN = 0.40, which corresponds to a P-value = 0.009 and as the value is 0.009, there is significant difference between the distributions at 99% confidence level. It is obvious that the results of the two tests are similar and the majority of the galaxies without PBLs tend to have smaller values of the gas to dust ratio. There are two reasons for this difference between the two types Sy2s. The objects without PBLs possess more dust close to the nuclear source and this obscuring material largely hides the core. On the other hand, it seems that the objects with PBLs have more powerful central engines on average, leading to higher $L_{[OIII]}$ (λ5007) luminosities, compared to those without PBLs.

Conclusion

Studying the sample of 82 Sy2 galaxies (34 with PBLs and 48 without detected PBLs) we have found that the Sy2s with PBLs reveal infrared properties more similar to the Sy1 galaxies. In this case the luminosity of the central source dominates over the host galaxy luminosity. It is why the Sy2 objects with PBLs occupy the area close to the line which represents the power-law locus on the (J–H) – (H–$\mathrm{K_S}$) diagram. The Sy2s without PBLs show infrared properties almost like normal galaxies. On the same color-color diagram these objects are located near the line which represents the black body locus. This fact indicates that there is a significant contribution of a stellar component of color similar to the normal galaxies. The reradiated by hot dust energy also has a considerable contribution. The main reasons for the more dominating host galaxy luminosity are highly obscured by dust central source and intrinsically weak central engine respectively. We have found that the Sy2's with PBLs have typically higher $F_{[OIII]}/F_{\mathrm{K_S}}$ ratios than the Sy2's without PBLs.

Acknowledgements. I would like to thank to R.S.Bachev, I.M.Yankulova and V.K.Golev for their helpful suggestions. This research has made use of the NASA/IPAC Extragalactic Database (NED) which is operated by the Jet Propulsion Laboratory, California Institute of Technology, under contract with the National Aeronautics and Space Administration. This research has made use of the NASA/ IPAC Infrared Science Archive, which is operated by the Jet Propulsion Laboratory, California Institute of Technology, under contract with the National Aeronautics and Space Administration. This research was supported by Contract DO 02-85 of the National Science Foundation in Bulgaria.

References

Antonucci, R., J. S. Miller, 1985, *ApJ, 297, 621*
Antonucci, R., 1993 ,*ARA&A, 31, 473*
Dahari, O., M. De Robertis, 1988, *ApJS, 67, 249*
Heisler, C. A., S. L. Lumsden, J. A. Bailey, 1997, *Nature, 385, 700*
Hyland, A. R., D. A. Allen, 1982, *MNRAS, 199, 943*
Kotilainen, J. K., M. J. Ward, C. Boisson, et al., 1992, *MNRAS, 256, 149*
Lumsden, S. L., C. A. Heisler, J. A. Bailey, et al., 2001, *MNRAS, 327, 459*
Moran, E. C., A. J. Barth, L. E. Kay, A. V. Filippenko, 2000, *ApJ,540, L73*
Moran, E. C., L. E. Kay, M. Davis, A. V. Filippenko, A. J. Barth, 2001, *ApJ,556, L75*
Nicastro F., Martocchia A., Matt G., 2003, *ApJ, 589, L13*
Panessa F., Bassani L., 2002, *A&A, 394, 435*
Peng, Z., Q. Gu, J. Melnick, Y. Zhao, 2006, *A&A, 453, 863*
Polletta M., Bassani L., Malaguti G., et al., 1996, *ApJS, 106, 399*
Shu X. W., Wang J. X., Jiang P., et al., 2007, *ApJ, 657, 167*
Shu X. W., Wang J. X., Jiang P., 2008, *ChJAA,8, 204*
Tran H. D., 2001, *ApJ, 554, L19*
Tran H. D., 2003, *ApJ, 583, 632*
Willner, S. P., M. Ward, A. Longmore, et al., 1984, *PASP, 96, 143*
Young, S., J. H. Hough, A. Efstathiou, et al., 1996, *MNRAS, 281, 1206*

Table 1. Data for 82 Sy2 galaxies with and without observed PBLs

Name	z	PBLs	J	H	Ks	$F_{\mathrm{K_s}}$	$F_{[OIII]}$	References
Circinus	0.0014	y	9.97	8.84	8.09	64.80	122.461	5
ESO 428-G014	0.0057	n	11.80	10.96	10.50	-	-	-
IC 3639	0.0109	y	12.34	11.57	11.11	4.02	34.0	1
IC 5063	0.0113	y	12.02	11.19	10.75	5.61	11.0	1
IC 5298	0.0274	n	12.98	12.13	11.55	2.69	17.0	2
IRAS 00198-7926	0.0728	n	14.31	13.50	12.53	1.08	0.884	1
IRAS 00521-7054	0.0689	n	14.17	12.96	11.80	2.14	2.872	4
IRAS 01475-0740	0.0177	y	14.28	13.50	12.98	0.72	6.248	2
IRAS 04103-2838	0.1175	n	15.19	14.30	13.78	-	-	-
IRAS 04210+0400	0.0450	n	14.76	13.98	13.02	0.69	4.502	4
IRAS 04229-2528	0.0418	n	14.37	13.60	13.14	0.62	1.442	4
IRAS 04259-0440	0.0155	n	14.14	13.43	13.05	0.68	13.0	1
IRAS 04385-0828	0.0151	y	13.44	12.55	11.80	2.13	0.693	4
IRAS 05189-2524	0.0426	y	13.43	12.33	11.17	3.80	13.0	1
IRAS 08277-0242	0.0406	n	13.95	13.19	12.72	-	-	-
IRAS 11058-1131	0.0548	y	13.96	13.12	12.42	1.21	3.32	4
IRAS 13452-4155	0.0386	n	13.93	13.13	12.50	-	-	-
IRAS 15480-0344	0.0303	y	13.31	12.50	11.95	1.86	10.942	2
IRAS 18325-5926	0.0200	y	12.59	11.50	10.50	7.04	54.223	5
IRAS 20210+1121	0.0564	n	14.08	13.32	12.75	0.89	21.082	4
IRAS 22017+0319	0.0611	y	14.25	13.28	12.41	1.22	3.608	4
IRAS 23128-5919	0.0446	n	13.78	13.02	12.48	1.14	0.851	4
MCG +1-27-020	0.0117	n	13.42	12.68	12.28	-	-	-
MCG -3-34-64	0.0165	y	12.26	11.47	11.00	4.48	40.0	1
MCG -5-23-16	0.0085	y	12.06	11.19	10.58	6.59	30.893	5
Mrk 1066	0.0120	n	12.44	11.57	11.05	4.26	29.695	3
Mrk 1210	0.0135	y	13.01	12.27	11.79	-	-	-
Mrk 1361	0.0226	n	13.51	12.65	12.06	1.67	18.0	2
Mrk 3	0.0135	y	11.82	11.00	10.53	6.89	360.175	3
Mrk 334	0.0219	n	13.09	12.16	11.46	2.93	20.0	1
Mrk 348	0.0150	y	13.05	12.21	11.60	2.57	26.026	2
Mrk 477	0.0377	y	13.96	13.29	12.77	0.88	101.235	3
Mrk 573	0.0172	y	12.71	11.95	11.51	2.79	30.15	2
NGC 1068	0.0038	y	9.91	8.95	7.91	76.46	470.0	1
NGC 1144	0.0288	n	12.62	11.72	11.26	3.50	2.767	2
NGC 1241	0.0135	n	12.34	11.51	11.10	4.08	6.719	2
NGC 1320	0.0089	n	12.24	11.42	10.94	4.72	4.83	2
NGC 1358	0.0134	n	12.11	11.33	10.94	-	-	-
NGC 1386	0.0029	n	11.41	10.59	10.13	9.90	50.486	2
NGC 1667	0.0152	n	12.26	11.45	11.05	4.26	31.858	2
NGC 1685	0.0152	n	13.50	12.75	12.35	1.29	0.156	3
NGC 2273	0.0061	y	11.87	11.04	10.58	-	-	-
NGC 2992	0.0077	y	11.85	10.91	10.36	8.04	33.386	3
NGC 3079	0.0037	n	11.71	10.55	9.81	13.37	5.55	2
NGC 3081	0.0080	y	12.06	11.27	10.87	5.03	10.686	3
NGC 3281	0.0107	n	12.14	11.28	10.75	-	-	-
NGC 3362	0.0277	n	13.44	12.68	12.33	1.31	1.131	2
NGC 34	0.0196	n	12.48	11.60	11.05	4.27	61.127	2
NGC 3660	0.0123	n	13.03	12.26	11.91	1.92	5.942	2
NGC 3982	0.0037	n	12.44	11.69	11.35	3.24	5.586	2
NGC 4117	0.0031	n	12.73	11.97	11.64	-	-	-
NGC 424	0.0118	y	12.55	11.49	10.46	7.34	17.059	2
NGC 4388	0.0084	y	12.20	11.29	10.78	5.47	22.0	1
NGC 4501	0.0076	n	11.08	10.27	9.83	13.08	0.523	2
NGC 4507	0.0118	y	12.03	11.18	10.61	6.41	7.824	3

Table 1. - Continued

Name	z	PBLs	J	H	K_S	F_{K_S}	$F_{[OIII]}$	References
NGC 4941	0.0037	n	12.02	11.24	10.86	5.09	36.419	2
NGC 513	0.0195	y	12.47	11.64	11.20	3.69	1.304	2
NGC 5135	0.0137	n	11.98	11.12	10.60	6.45	23.0	1
NGC 5194	0.0015	n	11.02	10.23	9.81	13.40	16.645	1
NGC 5252	0.0230	y	12.69	11.86	11.44	2.96	7.07	2
NGC 5283	0.0104	n	12.51	11.75	11.38	3.15	2.7	2
NGC 5347	0.0078	y	12.94	12.17	11.67	2.40	8.49	2
NGC 5506	0.0062	n	12.27	10.95	9.71	14.61	45.498	2
NGC 5643	0.0040	n	11.81	10.98	10.55	6.75	39.85	5
NGC 5695	0.0141	n	12.63	11.88	11.53	2.74	0.7	2
NGC 5728	0.0094	n	11.78	10.93	10.47	-	-	-
NGC 591	0.0152	y	12.85	12.07	11.70	-	-	-
NGC 5995	0.0252	y	12.25	11.29	10.56	6.69	66.0	1
NGC 6300	0.0037	n	11.82	10.95	10.43	7.50	1.487	5
NGC 6552	0.0265	y	13.21	12.43	11.97	1.82	13.009	2
NGC 6890	0.0081	n	12.31	11.51	11.10	4.08	5.898	2
NGC 7130	0.0162	n	12.36	11.55	11.07	4.17	52.097	2
NGC 7172	0.0087	n	11.94	10.96	10.33	8.25	0.4	1
NGC 7314	0.0048	y	12.87	12.07	11.58	2.62	102.849	5
NGC 7496	0.0055	n	12.74	11.96	11.58	2.62	4.256	2
NGC 7582	0.0053	n	11.44	10.42	9.62	15.93	50.21	1
NGC 7590	0.0053	n	11.95	11.17	10.80	5.38	1.519	2
NGC 7672	0.0134	n	13.66	12.86	12.57	-	-	-
NGC 7674	0.0289	y	13.01	12.13	11.35	3.24	17.0	1
NGC 7682	0.0171	y	12.93	12.18	11.82	2.10	6.302	2
NGC 788	0.0136	y	12.24	11.48	11.09	-	-	-
UGC 6100	0.0295	n	13.29	12.53	12.16	1.53	8.1	2

Note. In the columns are presented: the name of the galaxy; redshift z as reported in NED; detected PBLs (yes/no); J, H, K_S magnitudes in 6 arcsec aperture; F_{K_S} flux in units of 10^{-12} ergs s^{-1} cm^{-2}; the extinction-corrected flux $F_{[OIII]}$ in units of 10^{-13} ergs s^{-1} cm^{-2}; $F_{[OIII]}$ fluxes are taken from: (1) Lumsden et al. (2001), (2) Tran (2003), (3) Dahari and De Robertis (1988), (4) Young et al. (1996), (5) Polletta et al. (1996).